

ENHANCING AUTOMATIC CHORD RECOGNITION VIA PSEUDO-LABELING AND KNOWLEDGE DISTILLATION

Nghia Phan and Rong Jin

California State University, Fullerton

Gang Liu

Microsoft, Redmond, WA, USA

Xiao Dong

Beijing Normal-Hong Kong Baptist University

ABSTRACT

Automatic Chord Recognition (ACR) is constrained by the scarcity of aligned chord labels, as well-aligned annotations are costly to acquire. At the same time, open-weight pre-trained models are currently more accessible than their proprietary training data. In this work, we present a two-stage training pipeline that leverages pre-trained models together with unlabeled audio. The proposed method decouples training into two stages. In the first stage, we use a pre-trained BTC model [1] as a teacher to generate pseudo-labels for over 1,000 hours of diverse unlabeled audio and train a student model solely on these pseudo-labels. In the second stage, the student is continually trained on ground-truth labels as they become available. To prevent catastrophic forgetting of the representations learned in the first stage, we apply selective knowledge distillation (KD) from the teacher as a regularizer. In our experiments, two models (BTC, 2E1D) were used as students. In stage 1, using only pseudo-labels, the BTC student achieves over 99% of the teacher’s performance, while the 2E1D model achieves about 97% across seven standard `mir_eval` metrics. After a single training run for both students in stage 2, the resulting BTC student model surpasses the traditional supervised learning baseline by 2.5% and the original pre-trained teacher model by 1.1-3.2% across all metrics. The resulting 2E1D student model improves over the traditional supervised learning baseline by 2.67% on average and achieves almost the same performance as the teacher. Both cases show large gains on rare chord qualities.

1. INTRODUCTION

Automatic Chord Recognition (ACR) is a fundamental task in Music Information Retrieval (MIR) that aims to identify the harmonic content of audio recordings by outputting a sequence of chord labels. While large-scale labeled datasets are readily available for many machine learning domains, ACR faces significant data constraints: publicly available labeled chord datasets remain limited in both size and diversity [2]. This scarcity stems from the substantial manual effort required for precise audio-label alignment and consistent harmonic interpretation, as chord boundaries are inherently ambiguous and context-dependent [3, 4]. Furthermore, chord vocabularies are large and highly imbalanced; models excel on frequent major/minor chords but underperform on rare seventh and extended chords [2, 4, 5]. By training models only on scarce labeled data, we limit ourselves from making use of the unlabeled audio available in much larger quantities.

Hence, we use unlabeled audio to improve the training of chord recognition and show that the accuracy gains are disproportionately concentrated on rare chord qualities. For this purpose, we propose a two-stage training pipeline (see Figure 3). In the first stage, a

pre-trained teacher model generates pseudo-labels for over 1,000 hours of diverse unlabeled audio, and a student model is trained solely on these pseudo-labels until convergence, without requiring any ground-truth annotations. In the second stage, when labeled data becomes available, the pseudo-label-trained student is continually trained on ground-truth labels. To prevent catastrophic forgetting [6] of the representations acquired in the first stage, we apply selective knowledge distillation (KD) from the teacher as a regularizer throughout the second stage.

Prior semi-supervised ACR methods [5, 7] require ground-truth labels from the outset and fuse pseudo-labeled and labeled data together in a single training run. Our two-stage training approach decouples labeled and unlabeled data, making the training viable even when labeled data is initially unavailable. Notably, open-weight pre-trained models are often more readily available than their training data, offering a practical way to leverage teacher knowledge without access to proprietary datasets.

We also introduce a compact, dual-encoder architecture (2E1D) that is based on the Transformer architecture [8] and is lighter-weight than the teacher model. We demonstrate that our method can generalize across architectures. Our experiments show that the best resulting student surpasses both the traditional supervised learning training method and the pre-trained teacher model across all seven standard `mir_eval` metrics [9], with particularly large gains on rare chord qualities. A chord recognition web application is open-sourced¹, available for practitioners to experiment with and validate the performance of our models with their music audio locally.

2. RELATED WORK

Pseudo-labeling, where a trained model generates labels for unlabeled data, has become a cornerstone of semi-supervised learning [10]. The Noisy Student framework [11] demonstrated that iteratively training larger student models on pseudo-labeled data with noise injection can surpass teacher performance, establishing a paradigm for leveraging unlabeled data at scale. FixMatch [12] combined consistency regularization with pseudo-labeling using confidence thresholds, while Mean Teacher [13] introduced exponential moving averages of model weights for stable pseudo-label generation. Meta Pseudo Labels [14] further improved teacher-student training by jointly optimizing the teacher based on student feedback. Within MIR, pseudo-labeling has been successfully applied to various tasks including piano transcription [15], music tagging [16], and more broadly, speech recognition [17]. For ACR specifically, Bortolozzo et al. [5] adapted Noisy Student for rare chord recognition, employing confidence filtering and iterative teacher-student training to address class imbalance. Li et al. [7] applied contrastive learning to learn chord representations that trans-

Correspondence to: Nghia Phan <ptnghia@csu.fullerton.edu>
Preprint: Mar 28, 2026

¹<https://github.com/ptnghia-j/ChordMiniApp>

fer across datasets. However, these approaches typically require ground-truth labels from the outset and train on mixed pseudo-label and ground-truth signals within a single pipeline. In contrast, we investigate whether *separate* incremental learning stages can achieve comparable or superior performance by first training on pseudo-labels alone, then adapting to labeled data.

Transferring knowledge via temperature-scaled soft targets, or knowledge distillation (KD) [18], has been shown to provide richer supervision than hard labels. Beyond its original model compression goal, recent work has revealed KD’s regularization properties: soft labels reduce variance at the cost of introducing teacher bias [19]. Yuan et al. [20] studied conditions under which biased soft labels can still improve student generalization. Chen et al. [21] and Mansourian et al. [22] further demonstrated that KD acts as a regularizer against overfitting to noisy annotations. In continual learning, KD has been used to preserve prior knowledge while adapting to new data, mitigating catastrophic forgetting [23, 6]. Learning without Forgetting (LwF) [23] pioneered using distillation from the model’s own previous state to retain old knowledge when learning new tasks. Within MIR, KD has primarily served model compression, training smaller students to match larger teachers for efficient deployment [16]. We apply KD differently: as a regularization mechanism during continual learning that anchors the student to the teacher’s generalized representations. This preserves pseudo-label knowledge when ground-truth labels conflict with teacher predictions, while permitting adaptation when they align. Consequently, KD enables the student to refine decision boundaries without catastrophic forgetting.

Continual learning addresses the challenge of learning from non-stationary data streams without forgetting previously acquired knowledge [24]. In the MIR domain, this challenge is particularly relevant given the ongoing creation of new music and evolving annotation standards. While task-incremental and class-incremental scenarios have received significant attention, data-incremental continual learning remains underexplored for ACR. In this setting, the task and label space remain unchanged but new data arrive.

3. METHODOLOGY

3.1. Problem Formulation

Let $\mathcal{D}_l = \{(x_i, y_i)\}_{i=1}^{N_l}$ denote a small labeled dataset where $x_i \in \mathbb{R}^{T \times F}$ represents time–frequency features (e.g., Constant-Q Transform) with T frames and F frequency bins, and $y_i \in \{1, 2, \dots, C\}^T$ are frame-wise chord labels over a vocabulary of size C . Let $\mathcal{D}_u = \{x_j\}_{j=1}^{N_u}$ represent large-scale unlabeled datasets where $N_u \gg N_l$. Our objective is to train an effective student model f_s by leveraging pseudo-labels generated from \mathcal{D}_u . This mitigates reliance on expensive manual annotations while maintaining competitive performance.

3.2. Training Method

We employ a pre-trained teacher model $f_t : \mathbb{R}^{T \times F} \rightarrow \mathbb{R}^{T \times C}$ to generate pseudo-labels for unlabeled data. Any open-weight ACR model can serve as the teacher. In our experiments, we use the BTC model of Park et al. [1] as the teacher model, and adopt the standard vocabulary size $C = 170$ for all training settings. For each unlabeled sequence $x_j \in \mathcal{D}_u$, pseudo-labels are generated via frame-wise argmax over teacher outputs:

$$\hat{y}_j^{(t)} = \arg \max_{c \in \{1, \dots, C\}} [f_t(x_j)]_{t,c}, \quad t = 1, \dots, T \quad (1)$$

To preserve temporal coherence, we keep sequence boundaries intact during teacher inference (e.g., padding only at segment ends) and convert 100% of frames to pseudo-labels without confidence filtering, yielding a pseudo-labeled dataset:

$$\mathcal{D}_u^{(p)} = \{(x_j, \hat{y}_j)\}_{j=1}^{N_u} \quad (2)$$

Our method uses n complementary unlabeled datasets where $\mathcal{D}_u = \mathcal{D}_1 \cup \mathcal{D}_2 \cup \dots \cup \mathcal{D}_n$. The specific datasets used in our experiments are described in Section 4.1.

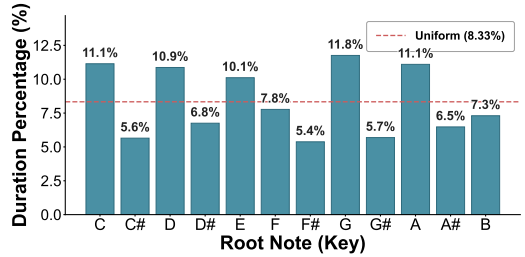


Figure 1: Duration-weighted chord root distribution across pseudo-labeled datasets. The dashed line indicates uniform distribution (8.33%). Pitch classes are well-represented with 98.4% uniformity.

3.2.1. Data Augmentation vs. Natural Chord Root Coverage

Supervised chord recognition systems typically require pitch-shifting augmentation to address severe chord root imbalance in labeled datasets. Studies show that widely-used datasets exhibit strong biases toward C and G major keys, often comprising over 30% of total duration, while enharmonically equivalent chords in other keys (e.g., F#, Db) remain underrepresented [2]. Without augmentation, models overfit to key-specific spectral patterns and fail to generalize chord templates across all 12 pitch classes. However, pitch-shifting introduces audible artifacts. Phase vocoder-based methods, including the Rubber Band library commonly used for music augmentation, produce transient smearing, phasiness, and spectral discontinuities [25]. These artifacts manifest as temporal blurring in Constant-Q Transform (CQT) features and artificial energy spreading across frequency bins (see Figure 2).

We observe that large-scale pseudo-labeling provides an alternative that eliminates pitch-shifting. We analyzed chord root distributions across 101,575 pseudo-labeled tracks (~1,072 hours) from FMA, DALI, and MAESTRO. As shown in Figure 1, all 12 pitch classes are well-represented with a coefficient of variation (CV) of 0.28, substantially lower than typical labeled datasets. The Shannon entropy reaches 3.53 bits (the maximum being 3.58 bits), corresponding to 98.4% uniformity. This natural coverage arises because diverse unlabeled corpora span multiple genres, artists, and production contexts, each contributing different key preferences that aggregate to near-uniform distribution. Consequently, pseudo-label pretraining exposes the model to patterns in all keys without requiring pitch-shifting augmentation. This avoids computational overhead and potential audio artifacts from signal manipulation.

3.2.2. The Training Pipeline

Figure 3 illustrates the complete two-stage training pipeline. In Stage 1, unlabeled data is first preprocessed into Constant-Q Transform spectrograms following the procedure described in Section 4.1.

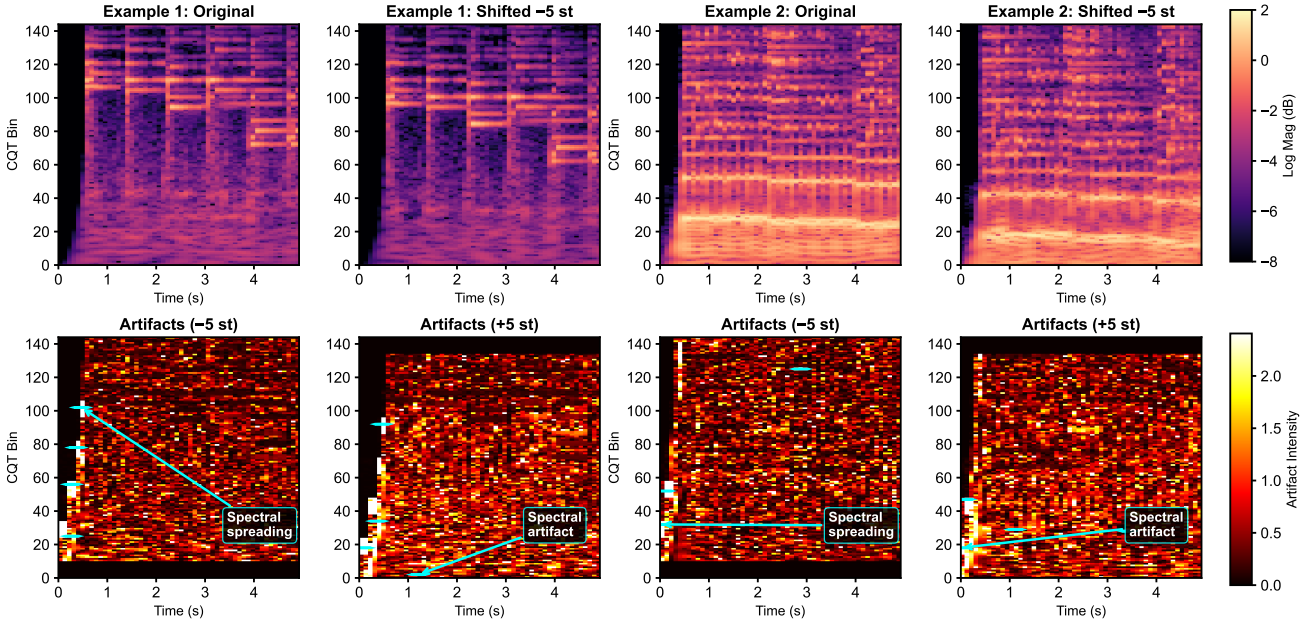


Figure 2: Constant-Q Transform (CQT) comparison revealing pitch-shifting artifacts. Top row: original and pitch-shifted (-5 semitones) spectrograms. Bottom row: artifact intensity maps for ± 5 semitones, computed by realigning shifted CQT bins to compensate for the intended frequency shift. Annotations indicate spectral spreading (low-frequency energy diffusion) and spectral artifacts (high-frequency noise) introduced by the phase-vocoder shift.

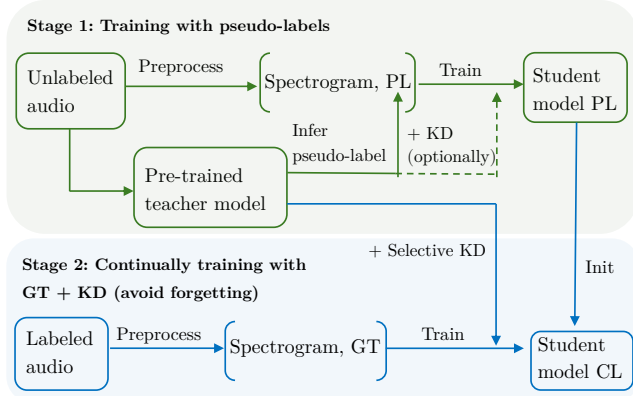


Figure 3: Illustration of the proposed two-stage training pipeline. Details of audio data are described in Section 4.1. Note: The resulting Student model CL from stage 2 can be continually trained when additional labeled data is available.

A pre-trained model is used as a teacher to infer frame-wise pseudo-labels (PL) on the unlabeled audio for each track, producing paired data (Spectrogram, PL). A student model is then trained on these pseudo-labeled pairs until convergence. Optionally, knowledge distillation (KD) from the teacher’s soft targets can be applied during this stage to accelerate convergence; this optional path is depicted as a dashed line in the figure. We denote the resulting model after the first stage of training as the *Student model PL*. Stage 2 begins when the labeled data becomes available. Labeled audio undergoes the same preprocessing, yielding paired data (spectrogram, GT),

where GT denotes ground-truth chord annotations. In this stage, *Student model PL* serves as the weight initialization for a new model called *Student model CL*. Then the *Student model CL* serves as the initialization for continual learning as additional labeled datasets are acquired. The selective KD signal, mentioned in Section 3.2.4, from the original pre-trained teacher is incorporated throughout the training on *Student model CL*. KD acts as regularization, anchoring the student to the teacher’s distributional knowledge when ground-truth labels conflict with teacher predictions, while still allowing adaptation when they agree. When KD is applied, the training loss is a weighted sum of a classification term and a KD term as follows:

$$\mathcal{L}_{\text{total}} = \alpha \mathcal{L}_{\text{KD}} + (1 - \alpha) \mathcal{L}_C \quad (3)$$

where $\alpha \in [0, 1]$ controls the balance between teacher regularization and label supervision, and \mathcal{L}_C denotes the classification loss. Specifically:

$$\mathcal{L}_C = \begin{cases} \mathcal{L}_{PL} = \frac{1}{|\mathcal{D}_u^{(p)}|} \sum_{(x, \hat{y}) \in \mathcal{D}_u^{(p)}} \ell_{CE}(f_s(x), \hat{y}) & \text{if Stage 1} \\ \mathcal{L}_{CE} = \frac{1}{|\mathcal{D}_l|} \sum_{(x, y) \in \mathcal{D}_l} \ell_{CE}(f_s(x), y) & \text{if Stage 2} \end{cases} \quad (4)$$

where $\mathcal{D}_u^{(p)}$ denotes the pseudo-labeled unlabeled data and \mathcal{D}_l denotes the ground-truth labeled data. Setting $\alpha=0$ reduces Eq. (3) to pure classification training without KD. The per-frame KD loss is:

$$\ell_{\text{KD}} = \tau^2 \cdot D_{\text{KL}}\left(\sigma\left(\frac{\mathbf{z}_t}{\tau}\right) \parallel \sigma\left(\frac{\mathbf{z}_s}{\tau}\right)\right) \quad (5)$$

where $\sigma(\cdot)$ denotes the softmax function, $\tau > 0$ is the temperature parameter that controls the smoothness of probability distributions, D_{KL} is the Kullback-Leibler divergence, and $\mathbf{z}_s, \mathbf{z}_t \in \mathbb{R}^C$ are the student and teacher logits, respectively.

3.2.3. KD as Regularization

We denote the temperature-softened probability distributions as $\mathbf{p}^{(s)} = \sigma(\mathbf{z}_s/\tau)$ and $\mathbf{p}^{(t)} = \sigma(\mathbf{z}_t/\tau)$, with $p_k^{(s)}$ and $p_k^{(t)}$ denoting the k -th class probability. The τ^2 scaling ensures gradient magnitudes remain comparable to cross-entropy [18]. The KD gradient with respect to student logits is:

$$\nabla_{\mathbf{z}_s} \mathcal{L}_{\text{KD}} = \tau (\mathbf{p}^{(s)} - \mathbf{p}^{(t)}). \quad (6)$$

This gradient ‘‘pulls’’ student predictions toward the teacher’s distribution. Combining with the classification term from Eq. (3):

$$\frac{\partial \mathcal{L}_{\text{total}}}{\partial z_{s,k}} = (1 - \alpha) \frac{\partial \mathcal{L}_C}{\partial z_{s,k}} + \alpha \tau (p_k^{(s)} - p_k^{(t)}). \quad (7)$$

The second term acts as a regularizer that anchors student predictions to the teacher’s distribution. When ground-truth labels conflict with teacher predictions (e.g., due to annotation noise or misalignment), this regularization prevents overfitting to erroneous labels. Conversely, when labels align with teacher predictions, the regularization does not impede adaptation. This property is particularly beneficial for ACR, where annotation inconsistencies are common due to subjective harmonic interpretation [3, 4].

3.2.4. Selective KD

To further improve robustness, we introduce *selective KD* that filters the teacher signal based on prediction confidence. Let $c = \max_i p_i^{(t)}$ denote the teacher’s maximum softmax probability. We define an asymmetric weighting function, $w(c) \in [0, 1]$ as:

$$w(c) = \begin{cases} 0 & \text{if } c < \theta_{\min} \\ 1 & \text{if } \theta_{\min} \leq c \leq \theta_{\max} \\ 1 - K \cdot \frac{c - \theta_{\max}}{1 - \theta_{\max}} & \text{if } c > \theta_{\max} \end{cases} \quad (8)$$

where θ_{\min} filters out uninformative low-confidence samples, θ_{\max} down-weights overconfident predictions that may bias toward majority classes, and factor $K \leq 1$ controls how overconfident predictions are down-weighted. The weighted KD loss becomes $\mathcal{L}_{\text{KD}}^{\text{sel}} = \frac{1}{N} \sum_i w(c_i) \cdot \ell_{\text{KD}}(x_i)$ over all N frames. Samples near decision boundaries (moderate confidence) contain valuable uncertainty information, so we preserve full weight in the informative range $[\theta_{\min}, \theta_{\max}]$. We apply selective KD throughout all Stage 2 continual learning experiments to stabilize training by reducing gradient variance from extreme-confidence samples. We set the hyperparameters with $\theta_{\min} = 0.1$, $\theta_{\max} = 0.9$, $K = 0.8$ as robust defaults based on the observed teacher-confidence distribution.

3.2.5. Experimental Models

BTC [1] serves as both the pseudo-labeling teacher and the baseline for self-distillation experiments. The model uses a direct frame projection followed by a stack of bi-directional transformer layers with position-wise feed-forward blocks, representing a *deeper* architecture with sequentially stacked attention layers.

For cross-architecture validation, we introduce a new compact dual-encoder architecture (2E1D)² for chord recognition that is purely transformer-based [8] (without any CNN layer). As shown in Figure 4, 2E1D adopts a *wider* design: (1) a frequency encoder that groups CQT bins into spectral clusters and applies self-attention

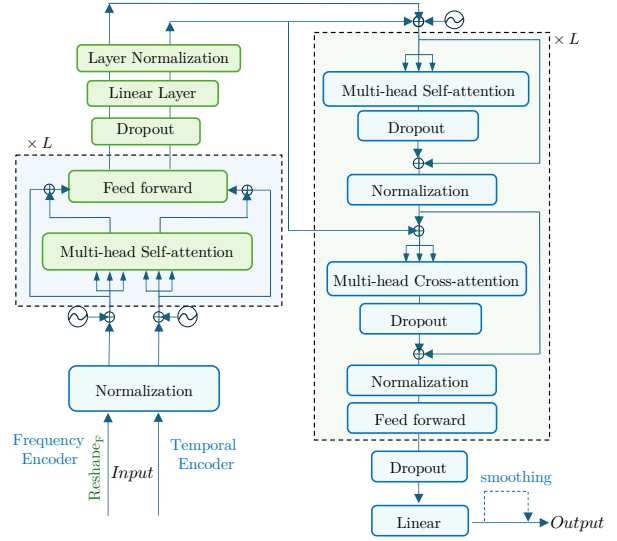


Figure 4: Experimental Dual Encoder Architecture (2E1D): The model consists of separate temporal and frequency encoders that process CQT features independently before fusion for chord classification.

to learn harmonic relationships across frequency bands; (2) a temporal encoder that processes full-band features to model chord progression patterns over time; and (3) a cross-attention fusion block that combines the two streams for final chord classification. At inference time, we apply a temporal smoothing pipeline over output logits to reduce frame-level prediction jitter. Each class logit channel is convolved with a normalized 1D Gaussian kernel $g[n] = \exp(-n^2/2\sigma^2)/Z$, where $\sigma = k/6$ follows the three-sigma rule for a kernel of width k , with replicate padding at segment boundaries. We further process the input using overlapping sliding windows with a stride of $s = \lfloor T(1 - r) \rfloor$, where T is the segment length and r is the overlap ratio, accumulating per-class votes across all windows before taking the frame-wise argmax.

The wider architecture design trades depth for parallel processing capacity: the 2E1D model generally runs faster than BTC. We investigate whether attention alone can capture both local spectral patterns and global temporal dependencies without CNN inductive biases [4, 26]. As shown in Section 5, the wider 2E1D architecture is more susceptible to degradation when adapting to noisy labels compared to the deeper architecture of BTC. Thus, the 2E1D model requires stronger KD regularization to maintain stability.

4. EXPERIMENTS

4.1. Datasets and Preprocessing

Unlabeled Datasets. We use three large-scale unlabeled datasets for pseudo-label generation, totaling over 1,000 hours of audio. The Free Music Archive [27] (\mathcal{D}_{FMA}) provides over 100,000 short-form tracks (~ 30 s) with extensive genre diversity. The MAESTRO dataset [28] ($\mathcal{D}_{\text{MAESTRO}}$) contributes over 200 hours of high-quality piano recordings with precise MIDI alignment. The DALI dataset [29] ($\mathcal{D}_{\text{DALI}}$) supplies over 5,000 full-length music tracks.

Labeled Datasets. We aggregate annotations from the Isophonics dataset [30], the McGill Billboard corpus [31], the RWC Pop [32],

²Model: <https://github.com/ptnghia-j/ChordMini>

and the USPop datasets [33], collecting a fixed subset of 600 songs. The dataset is then split in a ratio of 7:1:2 into train/validation/test sets (420/60/120 songs). The “50%” and “full” conditions in our continual learning experiments refer to using 210 and 420 training songs from this subset, respectively.

Clean vs. Noisy Annotations. To evaluate KD’s robustness to annotation noise, we prepare two versions of the labeled data: (1) *clean labels* with careful manual alignment, and (2) *noisy labels* sourced online without alignment correction, which primarily affect non-chord (“N”) label boundaries. This setup enables an ablation study of KD’s regularization effect under different noise conditions. **Preprocessing.** All audio undergoes identical preprocessing. The Constant-Q Transform features [34] are extracted with $F = 144$ frequency bins, 24 bins per octave, and a hop length of $h = 2048$ samples, yielding a temporal resolution of $\Delta t \approx 93\text{ms}$ at $f_s = 22.05\text{ kHz}$. Features undergo z-score normalization using teacher model statistics (μ_t, σ_t) to maintain identical input distributions.

4.2. Training Configuration

In the first stage, pseudo-labeling training employs the AdamW optimizer with a learning rate of 10^{-4} , a batch size of 256, and a sequence length of 108 frames (~ 10 seconds). The learning rate schedule incorporates warmup over 10 epochs to $3 \cdot 10^{-4}$, followed by cosine annealing decay. Early stopping monitors validation accuracy with a patience of 10 epochs. We reserve 10% of the pseudo-labeled data for validation and 10% as a held-out test set. In the second stage, continual learning, we use a reduced learning rate of 10^{-5} with decay upon observing a validation plateau. KD weight $\alpha=0.3$ balances adaptation and regularization. The temperature $\tau=3.0$ is empirically selected as the optimal value in all settings. Training continues until early stopping triggers. No data augmentation is applied in our two-stage pipeline (Section 3.2.1).

For the supervised learning (SL) baseline, both BTC and 2E1D are trained from scratch on the full labeled training set (420 songs). The SL baseline uses the same configuration as in pseudo-labeling training, except for the learning schedule. The learning rate decays at a rate of 0.9 when validation accuracy does not improve. Pitch-shifting augmentation via the Rubber Band library [25] transposes both audio and labels from -5 to $+6$ semitones.

4.3. Evaluation Metrics

We employ standard metrics from `mir_eval` library [9]. The Root metric compares the root note. The Thirds metric adds major and minor third intervals. The Triads metric evaluates all triadic qualities, while Majmin focuses on major and minor qualities. The Sevenths metric measures a predefined set of seventh chords. The Tetrads metric extends evaluation to four tones. MIREX considers an estimation accurate when at least three pitch classes are correct. Frame-wise accuracy (Acc), precision (Prec), recall (Rec), and F1 are computed using standard True Positive, False Positive, and False Negative counts. Additionally, we report Chord Symbol Recall (CSR) and Weighted Chord Symbol Recall (WCSR) following [5]:

$$CSR_{c,i} = \frac{|S_{c,i}^{pred} \cap S_{c,i}^{ref}|}{|S_{c,i}^{ref}|}, \quad WCSR_c = \frac{\sum_i T_i \cdot CSR_{c,i}}{\sum_i T_i} \quad (9)$$

where, for a chord class c and track index i , $S_{c,i}^{pred}$ denotes predicted chord labels, $S_{c,i}^{ref}$ denotes ground-truth labels for respective intervals, and T_i is the duration of the i -th track. The Average Chord

Quality Accuracy (ACQA), with the chord set C , is calculated as:

$$ACQA = \frac{\sum_{c \in C} WCSR_c}{|C|} \quad (10)$$

WCSR weights accuracy by class distribution, while ACQA gives equal weight to all chord qualities. This makes ACQA more sensitive to rare chord performance. Finally, for segmentation metrics, \mathcal{I}_{ref} and \mathcal{I}_{est} denote the sets of reference and estimated chord segment intervals, respectively. Over-segmentation (Over) measures how often predicted boundaries subdivide reference segments:

$$\text{Over} = \frac{\sum_{I \in \mathcal{I}_{ref}} \max_{J \in \mathcal{I}_{est}} |I \cap J|}{\sum_{I \in \mathcal{I}_{ref}} |I|} \quad (11)$$

Under-segmentation (Under) measures how often reference boundaries subdivide predicted segments:

$$\text{Under} = \frac{\sum_{J \in \mathcal{I}_{est}} \max_{I \in \mathcal{I}_{ref}} |I \cap J|}{\sum_{J \in \mathcal{I}_{est}} |J|} \quad (12)$$

The overall segmentation score (Seg) is defined as the minimum of the two directional scores, macro-averaged across N dataset tracks:

$$\text{Seg} = \frac{1}{N} \sum_{i=1}^N \min\{\text{Over}_i, \text{Under}_i\} \quad (13)$$

5. RESULTS

In this section, we present results for our two-stage training method across the metrics described in Section 4.3, including an ablation study on the KD regularization against noisy labels. All reported metrics are evaluated on the held-out test set (120 songs) from the clean labeled dataset described in Section 4.1.

5.1. Stage 1: Training with pseudo-labels

Increasing unlabeled data diversity consistently improves performance across the `mir_eval` metric hierarchy and segmentation quality (Table 1). Training on all three datasets (FMA, MAESTRO, DALI) yields the strongest results for both architectures, indicating that pseudo-label pretraining benefits from coverage of varied genres and recording conditions. Long-form datasets consisting of full-length tracks (DALI, MAESTRO) produce more stable pseudo-labels than short-form clips (FMA): DALI achieves higher frame-wise agreement with the teacher than FMA. Longer musical contexts provide consistent harmonic progressions, reducing boundary jitter and spurious chord predictions. However, FMA achieves better `mir_eval` results than DALI for 2E1D due to its larger size. The best BTC student reaches over 99% of teacher performance on ground-truth evaluation across all `mir_eval` metrics, while the purely transformer-based 2E1D achieves 96–98% of the teacher model results, demonstrating cross-architecture knowledge transfer. When all training targets are pseudo-labels, adding KD better aligns the student to the teacher’s soft-label distribution, resulting in improvements across frame-wise metrics despite a decrease in `mir_eval` metrics. In addition, KD accelerates optimization, as all pseudo-label training runs using KD converge in 30–40 epochs versus 50–70 for other settings; this comes with a modest training-time memory overhead to store and backpropagate full soft targets.

Model	Training Data	mir_eval Metrics							Segmentation			Frame-wise vs. teacher			
		Root	Thirds	Triads	7ths	Tetrads	Majmin	MIREX	Over	Under	Seg	Acc	Prec	Rec	F1
BTC [1]	Pre-trained weights	81.95	78.46	76.75	66.51	63.85	78.98	78.41	81.74	90.34	80.43	-	-	-	-
<i>Our two student models trained only with pseudo-labels (generated by the BTC teacher from unlabeled data)</i>															
2E1D (2.2M)	FMA (short-form)	77.28	73.70	72.15	61.78	58.94	74.49	73.68	83.55	83.96	78.03	57.27	34.43	20.29	23.51
	DALI (long-form)	74.32	65.53	63.73	52.68	50.27	65.91	65.37	77.09	85.92	74.00	78.25	48.06	37.41	39.52
	MAESTRO+DALI	79.50	75.80	74.11	63.18	60.28	76.53	75.50	83.14	84.85	78.53	79.44	52.23	41.95	44.50
	All (FMA+M+D)	80.37	76.63	74.91	64.37	61.50	77.29	76.35	84.34	85.63	80.15	80.15	57.01	45.20	47.49
	All + KD ($\alpha=0.3$)	80.17	76.36	74.68	63.93	61.06	77.09	76.08	84.23	85.27	79.69	81.23	58.14	46.33	48.62
BTC (3.03M)	FMA (short-form)	78.85	74.76	73.12	62.88	60.09	75.37	75.07	80.92	87.57	79.44	61.12	36.53	24.11	26.37
	DALI (long-form)	81.01	77.24	75.35	65.46	62.59	77.66	77.14	79.50	90.60	79.51	85.88	49.23	50.37	47.32
	MAESTRO+DALI	80.65	76.37	74.61	64.19	61.35	76.93	76.69	77.42	90.67	77.66	88.01	58.84	64.29	59.16
	All (FMA+M+D)	81.54	77.86	76.08	66.29	63.54	78.29	77.84	80.97	90.15	80.76	89.14	62.54	63.89	59.34
	All + KD ($\alpha=0.3$)	81.23	77.75	75.94	66.00	63.22	78.15	77.82	80.81	90.25	80.60	89.47	63.21	64.05	60.12

Table 1: Pseudo-labeling results across dataset configurations. The `mir_eval` metrics are computed against the ground-truth test set, while frame-wise accuracy, precision, recall, and F1 measure agreement with the teacher’s predictions. FMA contains short-form clips (~ 30 s), while DALI and MAESTRO provide long-form full tracks. The pre-trained BTC teacher [1] serves as the upper bound. Best results for BTC and 2E1D student models in the table are highlighted in blue and green, respectively.

5.2. Ablation: KD as Regularization

To understand KD’s role as a stabilizer under label noise, we evaluate continual learning with misaligned labels at varying α values (Table 2). Without KD ($\alpha=0$), both architectures suffer severe and consistent degradation across all metrics: BTC drops substantially throughout the recognition hierarchy, while the wider 2E1D collapses far more drastically to near-failure levels. The dual attention architecture is more susceptible to noisy label overfitting than the deeper BTC architecture. KD acts as an anchor, preventing noisy fine-tuning from destroying a good pseudo-label initialization. KD adds robustness without impeding adaptation. BTC peaks at $\alpha=0.3$ with a broad, consistent recovery across all metrics relative to the no-KD baseline, while 2E1D requires stronger regularization ($\alpha=0.5$) to stabilize. Figure 5 visualizes training dynamics. Without KD ($\alpha=0$), validation loss rises as the model overfits to noisy labels, whereas when $\alpha > 0$, KD anchors the student to the teacher’s distribution. This supports KD as an effective safeguard that preserves pseudo-label knowledge during adaptation.

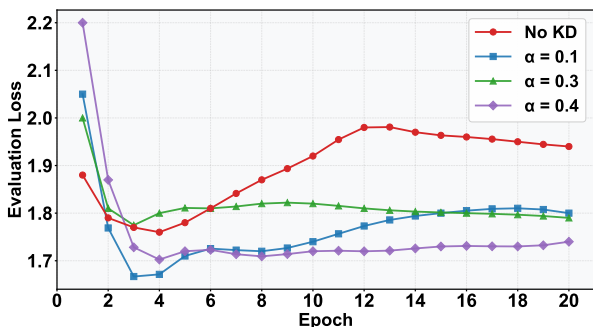


Figure 5: Evaluation loss of BTC model during continual training with different KD weights. Higher α values provide stronger regularization, mitigating performance degradation from noisy labels.

Model	α	Root	Thirds	Triads	7ths	Tetrads	Majmin	MIREX	Seg
2E1D	0	52.47	50.70	49.88	42.52	41.00	51.12	50.99	66.72
	0.1	55.85	54.16	53.41	47.68	45.78	54.88	54.07	67.70
	0.3	66.05	63.89	62.79	55.78	53.39	64.70	63.87	73.32
	0.5	74.21	71.25	69.78	61.20	58.35	72.09	71.54	76.84
	0.7	74.21	71.25	69.78	61.20	58.35	72.09	71.54	76.84
BTC	0	71.06	68.05	66.73	58.11	55.66	68.69	68.20	77.05
	0.1	73.88	70.86	69.43	60.91	58.25	71.52	70.96	78.59
	0.3	77.34	73.95	72.44	62.97	60.25	74.60	74.29	79.61
	0.4	76.95	72.88	71.30	61.30	58.57	73.59	73.18	78.98

Table 2: KD regularization effect during continual training with misaligned labels. The KD weight α controls the balance between teacher soft targets and ground-truth hard labels. BTC peaks at $\alpha=0.3$, while 2E1D requires stronger regularization. Best results for BTC and 2E1D are highlighted in blue and green, respectively.

5.3. Stage 2: Continually training with GT + KD

BTC with full labels surpasses both the teacher (Table 1) and the supervised learning (SL) baseline consistently across all seven `mir_eval` metrics. The 2E1D model similarly achieves broad improvements over its SL baseline. Among all metrics, 7ths and Tetrads benefit most from the combined effect of pseudo-label pre-training and ground-truth fine-tuning. Stage 1 supplies broad but biased coverage from diverse unlabeled audio, and Stage 2 corrects this bias using ground-truth labels. Crucially, KD does not prevent improvement when labels are clean (Table 3): models still surpass the teacher, indicating that KD selectively mitigates noise while preserving adaptation capacity. The complete two-stage pipeline demonstrates two key insights: (1) pseudo-label pretraining reduces labeled data requirements, as BTC can surpass the teacher with a small additional labeled dataset; and (2) gains are disproportionately concentrated on rare chord qualities, consistent with our scarcity motivation. The ACQA metric, which weights all chord qualities equally, reveals disproportionate gains: BTC improves by 10.5% from 29.0% to 39.5%, compared to only 3.0% improvement for distribution-weighted WCSR. This contrast strongly supports the observation that pseudo-label pretraining provides decision bound-

Method	mir_eval Metrics							Subset of Chord Quality Accuracy							Aggregate				
	Root	Thirds	Triads	7ths	Tetrads	Majmin	MIREX	Seg	Maj	Min	Dom7	Maj7	Min7	Dim	Dim7	Aug	Sus	WCSR	ACQA
<i>Prior Work (Noisy Student Framework)</i>																			
Bortolozzo et al. [5] †	–	–	–	–	–	–	–	–	55.5	54.4	51.0	12.0	47.5	30.4	43.3	–	–	46.8	24.5
Li et al. [7] †	78.05	73.56	70.71	61.11	56.84	74.64	74.26	–	–	–	–	–	–	–	–	–	–	–	–
<i>Traditional supervised learning (SL) baseline (trained on labeled data (full labels) with data augmentation)</i>																			
2E1D (SL) (2.2M)	79.39	76.14	74.53	64.53	61.67	76.89	76.24	78.50	91.7	62.1	23.9	25.2	44.4	3.5	0.0	0.0	8.0	68.7	24.4
BTC (SL) (3.03M)	81.52	78.00	76.12	65.93	63.44	78.11	77.79	79.38	88.7	63.1	36.7	28.2	52.8	23.3	0.0	5.9	22.9	68.6	29.0
<i>Results of our student models after Stage 2 with Data-Incremental Continual Learning (with clean labels, $\alpha=0.3$)</i>																			
2E1D (CL) (50%)	81.02	77.54	75.76	66.39	63.68	77.93	77.57	80.23	90.9	63.0	33.3	29.5	49.0	12.7	46.7	5.2	16.6	70.4	34.2
2E1D (CL) (full)	81.55	78.52	76.85	68.19	65.49	78.98	78.52	80.73	90.0	68.9	39.4	35.3	51.9	14.8	46.4	8.4	18.8	71.9	36.1
BTC (CL) (50%)	82.14	78.58	76.67	66.77	64.28	78.62	78.87	81.17	84.5	61.2	50.2	42.1	51.6	18.3	47.4	14.8	22.3	68.7	37.1
BTC (CL) (full)	83.03	80.17	78.33	69.38	67.00	80.24	80.16	81.71	87.1	65.6	51.6	42.3	55.7	23.5	45.6	18.5	25.5	71.6	39.5

Table 3: Data-incremental continual learning results with per-chord quality accuracy. After pseudo-labeling, we fine-tune on ground-truth labels with KD ($\alpha=0.3$). Our student BTC (CL) with full labels surpasses the teacher BTC shown in Table 1 across all mir_eval metrics. Two-stage pipeline significantly improves rare chord recognition (Dim, Dim7, Aug) compared to the supervised baseline. Best results for BTC and 2E1D are highlighted in blue and green, respectively. † We report only the metrics available in the original papers with our test set; cells not reported are left empty.

aries for rare chords that labeled datasets alone cannot establish. Figure 6 visualizes this effect. Major (45.5%) and Minor (22.3%) chords dominate the training distribution, while rare qualities (Dim: 1.8%, Dim7: 0.4%, Aug: 0.3%) constitute less than 3% combined. The SL baseline achieves 0% on Dim7 due to insufficient examples, while our pipeline leverages teacher pretraining to achieve 45.6%, a shift from failure to reasonable recognition.

Comparison to Prior Work. Table 3 demonstrates that the quality of pseudo-labels is a key factor in the performance of semi-supervised learning. Prior work [5, 7] relies on supervised models trained on limited labeled data to generate pseudo-labels. This constrains label quality and results in weaker model performance. In contrast, training with high-quality pseudo-labels generated by a better teacher model provides better-initialized weights, thereby creating a stronger starting point for model training and adaptation.

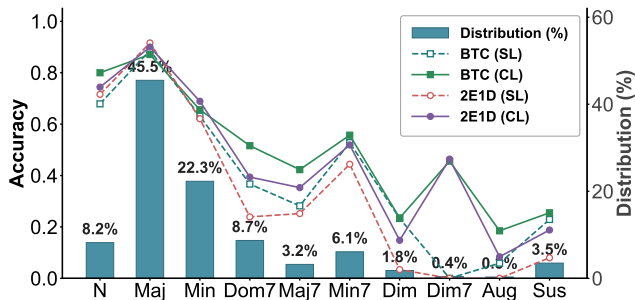


Figure 6: Chord quality distribution (bars) and recognition accuracy (lines) of models trained with traditional supervised learning approach (BTC (SL), 2E1D (SL)) versus our approach (BTC (CL), 2E1D (CL)).

6. CONCLUSION

Since model weights are often more readily available than proprietary training data, we present a practical training strategy for

the ACR problem that leverages open-weight pre-trained models when high-quality labels are scarce. We show that students trained solely on pseudo-labels can approach teacher-level performance across seven mir_eval metrics. We further demonstrate that continual learning can improve performance without catastrophic forgetting when the teacher provides sufficiently general representations. Under our pipeline, the best student model ultimately surpasses the teacher, especially on rare chord qualities (e.g., Dim, Dim7, Aug). Knowledge distillation improves robustness to noisy labels while preserving adaptability when ground-truth annotations are clean. We also find that the wider 2E1D architecture requires stronger KD regularization than the deeper BTC, underscoring how architectural choices influence continual-learning stability. A key limitation is reliance on teacher quality: biased or weakly generalizable teacher representations can transfer these shortcomings to the student. Future work will explore stronger teacher models and model architectures, ensembles of multiple teachers, scaling to additional unlabeled corpora, and extending the framework to related MIR tasks such as beat tracking and key estimation.

7. REFERENCES

- [1] J. Park, K. Choi, S. Jeon, D. Kim, and J. Park, “A Bi-directional Transformer for Musical Chord Recognition,” in *Proc. Int. Soc. Music Inf. Retrieval Conf. (ISMIR)*, Delft, The Netherlands, 2019, pp. 620–627.
- [2] E. J. Humphrey and J. P. Bello, “Four Timely Insights on Automatic Chord Estimation,” in *Proc. Int. Soc. Music Inf. Retrieval Conf. (ISMIR)*, Málaga, Spain, Oct. 2015, pp. 673–679.
- [3] C. Harte, “Towards Automatic Extraction of Harmony Information from Music Signals,” Ph.D. dissertation, Queen Mary, University of London, Aug. 2010.
- [4] J. Pauwels, K. O’Hanlon, E. Gómez, and M. B. Sandler, “20 Years of Automatic Chord Recognition from Audio,” in *Proc. Int. Soc. Music Inf. Retrieval Conf. (ISMIR)*, Delft, The Netherlands, Nov. 2019, pp. 54–63.

- [5] M. Bortolozzo, R. Schramm, and C. R. Jung, "Improving the Classification of Rare Chords With Unlabeled Data," in *IEEE Int. Conf. Acoustics, Speech and Signal Processing (ICASSP)*. IEEE, 2021, pp. 3390–3394.
- [6] R. M. French, "Catastrophic Forgetting in Connectionist Networks," *Trends in Cognitive Sciences*, vol. 3, no. 4, pp. 128–135, Apr. 1999.
- [7] C. Li, J. Jiang, Y. Li, and L. Tian, "Large-Vocabulary Chord Recognition Based on Contrastive Learning and Noisy Student," *IEEE Transactions on Consumer Electronics*, vol. 71, no. 2, pp. 3695–3706, Jul. 2024, early access published July 2024; print issue May 2025.
- [8] A. Vaswani, N. Shazeer, N. Parmar, J. Uszkoreit, L. Jones, A. N. Gomez, Ł. Kaiser, and I. Polosukhin, "Attention Is All You Need," in *Advances in Neural Information Processing Systems (NeurIPS)*, vol. 30, 2017, pp. 5998–6008.
- [9] C. Raffel, B. McFee, E. J. Humphrey, J. Salamon, O. Nieto, D. Liang, and D. P. W. Ellis, "mir_eval: A transparent implementation of common MIR metrics," in *Proc. Int. Soc. Music Inf. Retrieval Conf. (ISMIR)*, 2014, pp. 367–372.
- [10] D.-H. Lee, "Pseudo-label: The simple and efficient semi-supervised learning method for deep neural networks," in *ICML Workshop on Challenges in Representation Learning*, 2013.
- [11] Q. Xie, M.-T. Luong, E. Hovy, and Q. V. Le, "Self-training with Noisy Student improves ImageNet classification," in *Proc. IEEE/CVF Conf. Computer Vision and Pattern Recognition (CVPR)*, 2020, pp. 10 687–10 698.
- [12] K. Sohn, D. Berthelot, N. Carlini, Z. Zhang, H. Zhang, C. A. Raffel, E. D. Cubuk, A. Kurakin, and C.-L. Li, "FixMatch: Simplifying Semi-Supervised Learning with Consistency and Confidence," in *Advances in Neural Information Processing Systems (NeurIPS)*, vol. 33, 2020, pp. 596–608.
- [13] A. Tarvainen and H. Valpola, "Mean Teachers are Better Role Models: Weight-Averaged Consistency Targets Improve Semi-Supervised Learning Results," in *Advances in Neural Information Processing Systems (NeurIPS)*, vol. 30, 2017, pp. 1195–1204.
- [14] H. Pham, Z. Dai, Q. Xie, and Q. V. Le, "Meta Pseudo Labels," in *Proc. IEEE/CVF Conf. Computer Vision and Pattern Recognition (CVPR)*, 2021, pp. 11 557–11 568.
- [15] S. Strahl and M. Müller, "Semi-Supervised Piano Transcription Using Pseudo-Labeling Techniques," in *Proc. Int. Soc. Music Inf. Retrieval Conf. (ISMIR)*, 2024.
- [16] Y.-N. Hung, J.-C. Wang, M. Won, and D. Le, "Scaling up Musical Information Retrieval Training with Semi-supervised Learning," *arXiv preprint arXiv:2310.01353*, 2023. [Online]. Available: <https://arxiv.org/abs/2310.01353>
- [17] T. Likhomanenko, R. Collobert, N. Jaitly, and S. Bengio, "Continuous Soft Pseudo-Labeling in ASR," *arXiv preprint arXiv:2211.06007*, Nov. 2022, version v2.
- [18] G. Hinton, O. Vinyals, and J. Dean, "Distilling the Knowledge in a Neural Network," *arXiv preprint arXiv:1503.02531*, Mar. 2015.
- [19] L. S. Helong Zhou, "Rethinking soft labels for knowledge distillation: A bias–variance tradeoff perspective," *Proceedings of International Conference on Learning Representations (ICLR)*, 2021.
- [20] H. Yuan, N. Xu, Y. Shi, X. Geng, and Y. Rui, "Learning From Biased Soft Labels," *arXiv preprint arXiv:2302.08155*, Feb. 2023.
- [21] D. Chen, "A Note on Knowledge Distillation Loss Function for Object Classification," *arXiv preprint arXiv:2109.06458*, Sep. 2023, version v3.
- [22] A. M. Mansourian, R. Ahmadi, M. Ghafouri, A. M. Babaei, E. B. Golezani, Z. yasamani ghamchi, V. Ramezani, A. Taherian, K. Dinashi, A. Miri, and S. Kasaei, "A comprehensive survey on knowledge distillation," *Transactions on Machine Learning Research*, 2025.
- [23] Z. Li and D. Hoiem, "Learning without Forgetting," *IEEE Trans. Pattern Anal. Mach. Intell.*, vol. 40, no. 12, pp. 2935–2947, Dec. 2018.
- [24] G. M. van de Ven and A. S. Tolias, "Three Scenarios for Continual Learning," *arXiv preprint arXiv:1904.07734*, 2019.
- [25] J. Driedger and M. Müller, "A Review of Time-Scale Modification of Music Signals," *Applied Sciences*, vol. 6, no. 2, p. 57, 2016.
- [26] H. H. Fard, "Automatic Chord Recognition with Fully Convolutional Neural Networks," Master's thesis, Technische Universität Berlin, Sep. 2020.
- [27] M. Defferrard, K. Benzi, P. Vandergheynst, and X. Bresson, "FMA: A Dataset for Music Analysis," in *Proc. Int. Soc. Music Inf. Retrieval Conf. (ISMIR)*, 2017, pp. 316–323. [Online]. Available: <https://arxiv.org/abs/1612.01840>
- [28] C. Hawthorne, A. Stasyuk, A. Roberts, I. Simon, C.-Z. A. Huang, S. Dieleman, E. Elsen, J. Engel, and D. Eck, "Enabling Factorized Piano Music Modeling and Generation with the MAESTRO Dataset," in *Proc. Int. Conf. Learning Representations (ICLR)*, 2019.
- [29] G. Meseguer-Brocal, A. Cohen-Hadria, and G. Peeters, "DALI: A Large Dataset of Synchronized Audio, Lyrics and Notes, Automatically Created Using Teacher-Student Machine Learning Paradigm," in *Proc. Int. Soc. Music Inf. Retrieval Conf. (ISMIR)*, Paris, France, 2018.
- [30] M. Mauch, C. Cannam, M. Davies, S. Dixon, C. Harte, S. Kolozali, D. Tidhar, and M. Sandler, "Omras2 Metadata Project 2009," in *Proc. Int. Soc. Music Inf. Retrieval Conf. (ISMIR)*, Kobe, Japan, Oct. 2009.
- [31] J. A. Burgoyne, J. Wild, and I. Fujinaga, "An Expert Ground Truth Set for Audio Chord Recognition and Music Analysis," in *Proc. Int. Soc. Music Inf. Retrieval Conf. (ISMIR)*, Miami, Florida, USA, Oct. 2011, pp. 633–638.
- [32] M. Goto, H. Hashiguchi, T. Nishimura, and R. Oka, "RWC Music Database: Popular, Classical and Jazz Music Databases," in *Proc. Int. Soc. Music Inf. Retrieval Conf. (ISMIR)*, Paris, France, Oct. 2002, pp. 287–288.
- [33] B. McFee and J. P. Bello, "Structured Training for Large-Vocabulary Chord Recognition," in *Proc. Int. Soc. Music Inf. Retrieval Conf. (ISMIR)*, Suzhou, China, Oct. 2017, pp. 188–194.
- [34] C. Schörkhuber and A. Klapuri, "Constant-Q Transform Toolbox for Music Processing," in *Proc. Sound and Music Computing Conf. (SMC)*, Barcelona, Spain, Jul. 2010, pp. 3–64.